附件一

行政院國家科學委員會補助專題研究計畫 ■ 成 果 報 告 □ 期中進度報告

（計畫名稱）

低成本高性能高可靠度先進氧化鋅奈米線場發射元件之研究

計畫類別：■ 個別型計畫　　□ 整合型計畫
計畫編號：NSC 97－2221－E－009　－150-MY3
執行期間：　99　年　8　月　1　日至　100　年　7　月　31　日

計畫主持人：曾俊元
共同主持人：
計畫參與人員：

成果報告類型(依經費核定清單規定繳交)：□精簡報告　■完整報告

本成果報告包括以下應繳交之附件：
□赴國外出差或研習心得報告一份
□赴大陸地區出差或研習心得報告一份
□出席國際學術會議心得報告及發表之論文各一份
□國際合作研究計畫國外研究報告書一份

處理方式：除產學合作研究計畫、提升產業技術及人才培育研究計畫、列管計畫及下列情形者外，得立即公開查詢
□涉及專利或其他智慧財產權，□一年□二年後可公開查詢

執行單位：國立交通大學
中　華　民　國　100　年　10　月　10　日

摘要

本研究進行氧化鋅奈米柱陣列製備、光學與場發射特性的探討，主要利用兩種方式去改善氧化鋅奈米柱陣列的場發射特性：鎵摻雜和氧氣電漿蝕刻處理形成氧化鋅奈米尖錐，在上述的兩種方法中，皆可顯著的降低啟動電場與增加場效增益因子。氧化鋅奈米柱陣列的形貌、晶體結構和組成主要利用 X 光繞射、場發射掃瞄電子顯微鏡、場發射穿透式電子顯微鏡和能量分佈分析儀得知，其結果顯示奈米柱具有高優選 C-軸成長方向且組成符合當量化，螢光光譜分析結果指出在經由鎵摻雜和氧氣電漿蝕刻皆可填補氧化鋅奈米柱陣列本身的氧空缺，使其具備有較佳的結晶性。最終結合鎵摻雜（鎵/鋅反應溶液中莫爾比為 1 %）和氧氣電漿蝕刻處理(蝕刻時間為 60 秒)所製備的鎵摻雜的氧化鋅奈米尖錐(角度約 100 度）其啟動電場為 1.99 V/μm、場效增益因子達 2465 且可穩定的操作達 2×10^4 秒，我們認為氧化鋅奈米柱先藉由鎵摻雜降低本身的功函數後再經由氧氣電漿處理形成奈米尖錐的形貌，使得電子更容易發射，場發射特性因而顯著的提升。對於溫度變化造成鎵摻雜的氧化鋅奈米尖錐的場發射特性穩定度進行量測，其結果顯示出鎵摻雜的氧化鋅奈米尖錐可於 25 ℃至 100 ℃穩定操作達 3000 秒。因此，我們認為鎵摻雜的氧化鋅奈米尖錐在未來對於場發射顯示器與照明元件方面的應用具備有高度的可行性。

關鍵字：鎵摻雜的氧化鋅、氧氣電漿處理、場發射特性

Abstract

The fabrication, optical and field emission properties of ZnO-based nanorod emitters were studied. Two novel methods involving gallium doped ZnO nanorods and formation of tip structure on the top of ZnO nanorod by oxygen plasma treatment are employed to improve the field emission properties of the nanorod emitters. By either of these two methods, the nanorod emitters exhibit significantly reduced turn-on field and enhanced field emission factor. The morphology, crystal structure and composition of all the nanorods for making emitters are characterized by scanning electron microscopy, X-ray diffraction and energy dispersive X-ray spectrometer. The nanorods exhibit the highly preferred c-axis orientation single crystal structure. The photoluminescence spectra indicate the nanorods have better crystalline structure after doping and oxygen plasma treatment. Combination gallium doping process (Ga/Zn molar ratio of 1 % in solution) and oxygen plasma treatment (etching time of 60 sec), the tip structured Ga-doped ZnO (GZO) nanorod emitters with tip angle of 100° have a turn-on field of 1.99 V/μm under a current density of 1 $\mu A/cm^2$, field enhancement factor of 2465 and stable operation over 2×10^4 sec. Such improved field emission properties are attributed to decreased work function and sharp nanotips morphology. In addition, the GZO nanorod emitters with tip structure are successively and stably operated between the 25 ℃ and 100 ℃ over 3000 sec based on the high temperature field emission measurement results. They have high potential for practical applications in flat panel display and light emitting device in the future.

Keyword: Ga-doped ZnO, Oxygen plasma treatment, Field emission properties

1. *Introduction*

One-dimensional (1D) semiconductor nanostructures attract renewed interest because of their excellent optoelectronic properties and promising applications[1-2]. Among the various applications, field emission displays had attracted a lot of interest for their high aspect ratio, proper number densities, and high emission stability[3]. Several groups have been reported on field emission from nanorods / nanowires such as carbon nanotubes (CNTs)[4], diamond cones[5], $Ni_{31}Si_{12}$ nanowires[6] and ZnO nanorods[7-8] etc. Among 1D nanostructure, the ZnO nanorods is considered to be one of the most promising cold cathode materials due to their large exciton binding energy, strong radiation-oxidation resistance, and high thermal stability[9-10]. Generally, the field emission property depends on the material work function, tip morphology and number density of nanorod emitters. But, still it's a challenge to develop the nanorod emitters at a particular areas. Therefore, improvement of the field emission performances is an important issue for their application in field emission displays.

It is well known that structural properties and dopants may determine the electronic properties of the materials. The typical dopants that have been used to enhance the carrier concentrations of ZnO are the group Ⅲ (Al, In and Ga) and group Ⅳ (Sn) elements[11-15]. Among those elements, gallium is an effective dopant for reducing the resistivity, less lattice distortion and more resistant to oxidation than Aluminum. Various methods including metal organic chemical vapor deposition and thermal evaporation[16-17], have been reported to synthesize GZO nanorods. However, those methods required high temperature, limitation for the device applications. Therefore, we synthesis GZO nanorods by the solution method which has the advantages of lower synthesis temperature (90 ℃) and larger scale production. The effects of gallium doping on the field emission and photoluminescence properties of GZO nanorod emitters are investigated.

On the other hand, it is necessary to control the morphologies of the nanorods to improve their field emission properties because the vertically aligned ZnO nanorods have relatively large diameter and hexagonal structure at top end. Plasma treatment is an easy and fast process to control morphology of the nanorods and we recently reported the preparation of ZnO nanotip structures from the as-grown ZnO nanorods by using the combination of chemical etching and Ar plasma treatment[18]. However, there are no literature that has ever been reported on the effect of oxygen plasma treatment on field emission properties of ZnO nanorods. In this paper, we synthesized the Ga-doped ZnO nanorods by using solution method and employed oxygen plasma etching method to form nanotip on the as-grown nanorods. Effects of etching time on morphology of nanostructures, electrical and optical characteristics of ZnO nanorods are also investigated.

2. *Experimental method*

GZO nanorod with different Ga/Zn molar ratios were grown by an aqueous solution method in 70 ml solution containing 0.05 M zinc nitrate hexahydrate ($Zn(NO_3)_2 \cdot 6H_2O$, 99.9% purity), 0.05 M methenamine ($C_6H_{12}N_4$, 99.9% purity), and 0, 0.2, 1 and 2 % gallium nitrate hydrate

($Ga(NO_3)_3 \cdot xH_2O$, 99.9% purity), respectively. The substrates were placed downward in the above solutions at 90 ℃ for 2 h to grow the nanorods. After the reaction, the substrates were removed respective from the solution, rinsed with deionized water thoroughly and dried using nitrogen.

For making the nanorods with tip morphologies, nanorods were bound on a sputtering target by carbon tape and exposed to oxygen plasma for 0, 30, 60 and 120 sec, respectively. For the plasma treatment, process pressure and rf-power were maintained at $5x10^{-2}$ Torr and 30 W, respectively.

The morphology, size distribution and crystal structure of all the nanorods were investigated by a field-emission scanning electron microscope (FE-SEM, Hitachi S-4700I), a transmission electron microscope (TEM, JEOL 2100F), and a X-ray diffractor (XRD, Bede D1). The chemical composition was estimated by a energy dispersive X-ray spectrometer (EDS, Oxford ISIS300). The field-emission current-voltage (I-V) curves of all nanorod emitters were measured at a pressure of 2×10^{-6} Torr kept by a turbo molecular pump. A copper tip was employed to act as an anode with the tip area of 7.09×10^{-3} cm^2 and p-type Si covered with ZnO emitters as an cathode with an area of $1cm^2$. We used micrometer (accuracy of ±1 μm) to adjust the distance between a copper anode and nanorod emitters. The distances of the as-grown and other nanorod emitters with the anode are 100 and 150 μm, respectively. The field emission properties are affected by the anode area and anode-cathode distance based on Filips model[19]. The turn-on and threshold fields are defined at current densities of 1 $\mu A/cm^2$ and 1 mA/cm^2, respectively. The dependence of the field emission current on the anode-cathode voltage was recorded using programmable Keithley 237 picoammeter measurement system. The stability measurements were also carried out for the GZO nanorod emitters at temperature of 25, 50 and 100 ℃, respectively. The photoluminescence (PL) spectra were obtained using a He-Cd laser (325nm) as excitation source at room temperature.

3. *Results and discussion*

Figures 1(a-d) show the FE-SEM morphologies of as-grown ZnO and GZO (Ga/Zn molar ratios of 0.2, 1 and 2 % in solution, respectively) nanorod emitters. It can be observed that the small quantities of gallium doping would not significantly influence the length and diameter of the nanorod emitters. However, for the nanorod prepared with the solution of 2 % Ga/Zn molar ratio, it shows very different morphology, significant reduction of number density, length and diameter (Figure 1(d)).The higher amount of gallium doping has a great impact on the size, morphology and number density of the nanorod emitters. The ZnO nanorods are formed by two different processes: nucleation and growth. The reactions can be explained as follows[20-21]:

$$(CH_2)_6N_4 + 6H_2O \rightarrow 6HCHO + 4NH_3 \quad (1)$$

$$NH_3 + H_2O \rightarrow NH_4^+ + OH^- \quad (2)$$

$$4OH^- + Zn^{2+} \rightarrow Zn(OH)_4^{2-} \quad (3)$$

$$Zn(OH)_4^{2-} \rightarrow ZnO_{(s)} + H_2O + 2OH^- \quad (4)$$

In our experiment, ZnO nanorod synthesis was performed in a closed system, that is, a limited amount of ZnO precursor in a specific period of time. As the Ga/Zn molar ratio at the solution is increased, the additional gallium ions prefer to react with the OH^- at the solution. This reaction reduces the ZnO precursor at the nucleation sites[22]. Therefore, the number density of ZnO nanorod arrays is decreased as the gallium nitrate concentration increases.

Figures 1(e-g) show the FE-SEM morphologies of the oxygen plasma treated (etching times of 30, 60 and 120 sec, respectively) ZnO nanorod emitters. The morphology of ZnO nanorod emitters reveals dramatic change due to the oxygen plasma treatment. While oxygen plasma treatment for 30 sec, we find that the top of the nanorods becomes tower-shaped morphology. By increasing the treatment time to 60 sec, the tip structure of the ZnO nanorod emitters is formed. The formation of acute nanotips morphology is due to the oxygen ion bombardment at the edge of the nanorods leading to isotropic etching[18]. Figure 1(g) shows the morphology of the nanorods plasma treated for 120 sec, indicating a destruction due to over etched and a decrease of aspect (c/a) ratio of the nanorods, which will degrade the performance of the emitters[23].

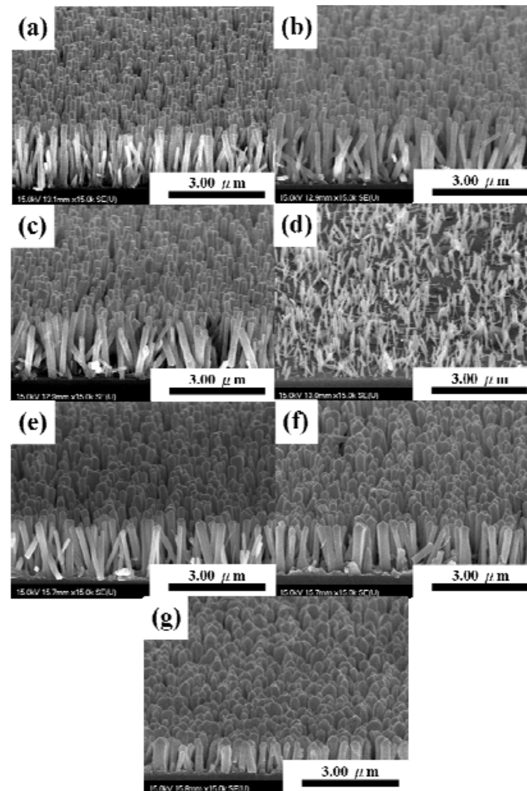

Figure 1 Typical FE-SEM images of ZnO nanorod with various Ga/Zn molar ratios in solution (a) 0 % (as-grown), (b) 0.2 %, (c) 1 %, (d) 2% and various oxygen plasma treatment times (e) 30 sec, (f) 60 sec and (g) 120 s. respectively.

Figures 2(a-b) show the XRD spectra of the as grown ZnO, GZO and various oxygen plasma etched ZnO nanorod emitters. It indicates that all the nanorods belong to the single phase hexagonal wurtzite structure with preferred (002) orientation. Figure 2(a) depicts that the (002) peak shifts to high angle (from 34.3° to 34.6°), as Ga/Zn ratio changed from 0 to 2 % because the

ionic radius of gallium ion (0.62 Å) is smaller than that of zinc ion (0.74 Å). However, the intensity of (002) orientation peak of GZO (Ga/Zn molar ratio of 2 %) nanorods is reduced probably due to lattice distortion caused by the larger amount of gallium ions. Figure 2(b) shows that the intensity of the (002) diffraction peak increases with an increase of the oxygen plasma bombardment time up to 120 s. It indicates that the oxygen ions bombardment not only helps to form tip structure but also oxidizes of the oxygen vacancies at the ZnO nanorods.

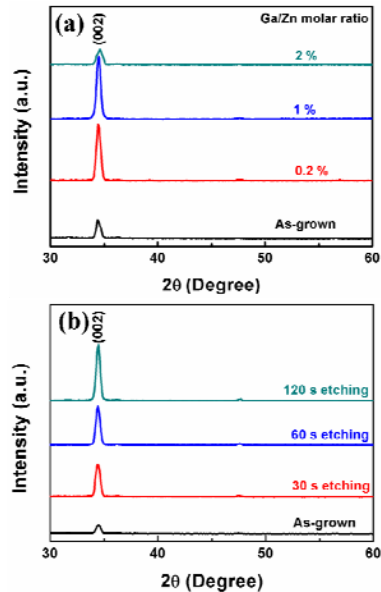

Figure 2 XRD analysis of (a) GZO nanorod with various Ga/Zn molar ratios in solution and (b) ZnO nanorod emitters with the various oxygen plasma eching times.

The crystalline properties and morphology of the nanorods have been studied using plane view TEM observations. The bright field images, selected area electron diffraction (SAED) pattern and EDS analysis of the as-grown ZnO, GZO (Ga/Zn molar ratio of 2 %) and as-grown ZnO after oxygen plasma treatment for 60 s nanorods are shown in Figures 3(a-f), respectively. The (002) c-axis interplanar spacing is 2.56 Å (insets in Figures 3(a) and (c)), which is consistent with the XRD results. The SAED patterns (insets in Figures 3(a) and (c)) observe that the preferred growth of the nanorod is in the [0001] direction. The typical EDS spectrum (Figure 3(b)), indicates the as-grown nanorods are composed of only Zn and O. No evidence of other impurities is found from the spectrum. With further quantitative analysis of EDS, it reveals that the atomic ratio of Zn/O is 49.13:50.87, which is close to stoichiometric ratio. The EDS spectrum (Figure 3(d)) for the GZO nanorods reveals that the atomic ratio of Ga/Zn is 1.73±0.11 %. Table (1) lists the comparison between Ga/Zn molar ratios in the solution and measured Ga/Zn atomic ratio. It shows no significant differences between them, which confirms the successful doping of gallium ions into ZnO nanorods by solution method. Figure 3(e) shows that the nanorod has a small tip, which is consistent with the result of FE-SEM observation and the tip angle approximately 100° can be obtained. The SAED pattern (insets in Figure 3(e)) show the preferred [0001] growth of the ZnO nanorods. A high resolution images shown in insets of Figure 3(e) reveals the tip and side of nanorods have lattice planes with interplaner spaces of 2.54 Å and 2.58 Å, respectively, indicating the ZnO nanorods are wurtzite structure with [0001] direction. It is

also observed that the tip area is smooth surface and no crack, indicating that the oxygen plasma treatment is a fast and powerful nanoscale surface modification method. The EDS spectrum shown in Figure 3(f) indicates that the constituent elements of the nanorod are only composed of Zn and O having atomic ratio of Zn/O is 48.7:51.3.

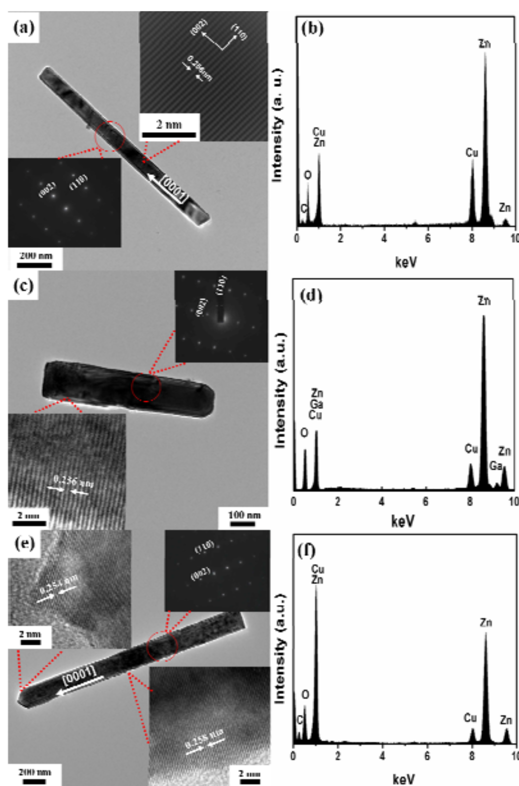

Figure 3 TEM bright field image, corresponding SAED pattern, HR-TEM image and EDS analysis of different nanorod: ((a) and (b)) as-grown ZnO, ((c) and (d)) GZO (Ga/Zn molar ratio of 2 %) and ((e) and (f)) as-grown ZnO nanorod after 60 sec oxygen plasma etching.

The room-temperature PL spectra of **the** as-grown ZnO, GZO and oxygen plasma etched ZnO nanorod emitters are shown in Figures 4(a-b). The strong UV emissions for those nanorods occur at about 378 nm, which comes from the recombination of exciton. The broad emission bands located at about 550 nm, which is the green emission of the visible spectrum. These peaks occur from the oxygen vacancies of the nanorods[24-25]. The inset of Figure 4(a) indicates that the peaks are red-shifted (from 377 to 379 nm) with an increase of gallium doping level. A similar red shift was also observed in Ga-, In- and Sn-doped ZnO nanowires[14-15]. The gallium doped into ZnO nanorods significantly increases the free electron density, as a result renormalization of the band gap and thus leading to a red-shift of the optical transitions. It is known that oxygen vacancies are the common defect in n-type ZnO, which are relative to visible emission. Figures 4(a-b), indicate the intensity of visible emission decreases, due to the decrease in oxygen vacancy concentration by gallium doping and oxygen plasma treatment. Previously, the reduced oxygen vacancy concentration of ZnO nanorods by annealing at various temperatures in an oxygen atmosphere was reported[26]. Thus, the reduced green emission is expected to occur by annealing at oxygen atmosphere. Inset of Figure 4(b) shows green emission the peak intensity decreases,

indicating clearly the decreased oxygen vacancy concentration and consequently, the enhanced intensity of UV emission during oxygen plasma treatment occurred.

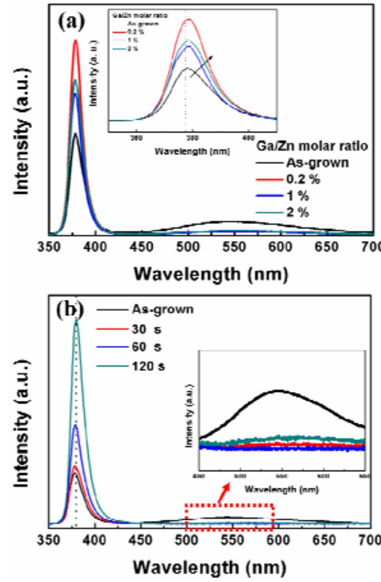

Figure 4 Room temperature PL spectra of (a) GZO nanorod with various Ga/Zn molar ratios in solution (inset show magnify of UV emission areas) and (b) ZnO nanorod emitters with the various oxygen plasma etching times (inset show magnify of green emission areas).

It was reported that the gallium doped into ZnO nanorods provide much higher electron concentration with reduction of resistivity and lowers the voltage drop at the nanorod emitters[27]. On the other hand, the n-type doping can increase the possibility of electrons tunneling by lifting the Fermi level and reduced the work function of the nanorod emitters. We measured the carrier concentration of gallium doped ZnO nanorods (as listed in Table 1) by traditional Hall Effect measurement. The relation between electron concentration and the Fermi level can be written as[28]

$$n = 2\left(\frac{2\pi m^* kT}{h^2}\right)^{1.5} \exp\left[-\frac{(E_F - E_C)}{KT}\right] \qquad (5)$$

Where n is carrier concentration, m* the electron effective mass, k Boltzmann constant, T the absolute temperature, h the Plank's constant, E_F and E_C are energies at the Fermi level and bottom of conduction band, respectively. Using the carrier concentration (n), $m^*=0.23\ m_0$ (m_0 is the electron static mass) and $E_C=4.35$ eV for ZnO, the work functions of the GZO nanorod emitters with 0.2, 1, and 2 % of Ga/Zn molar ratios in the solution are estimated to be 4.65, 4.57, and 4.56 eV, respectively.

Figures 5 (a) and (c) show the J-E curves of the as-grown ZnO, GZO and oxygen plasma etched ZnO nanorod emitters. The field emission current–voltage characteristics are analyzed by using the Fowler-Nordheim (F-N) equation[19, 29]:

$$J = A\left(\frac{\beta^2 E^2}{\varphi}\right) \exp\left(-\frac{B\varphi^{1.5}}{\beta E}\right) \qquad (6)$$

$$\ln(\frac{J}{E^2}) = \ln(\frac{A\beta^2}{\varphi}) - \frac{B\varphi^{1.5}}{\beta E} \quad (7)$$

Where J is the current density, E the applied electric field, $A=1.56\times10^{-10}$ (AeV/V^2), $B=6.83\times10^9$ ($V/eV^{1.5}m$), β a field enhancement factor and φ the work function of the emitter. When the work functions of the ZnO and GZO nanorods are known, the field enhancement factor can be calculated from the slope of the F-N plots and shown in Figures 5(b) and (d). The field emission properties of the nanorods with various Ga/Zn molar ratios at the solutions and different oxygen plasma treatment times are listed in Tables 1 and 2. With increase the Ga/Zn molar ratio in solution, it also increase carrier concentration and reduces the turn-on field of the nanorod emitters. The GZO nanorods prepared with Ga/Zn of 1 % in solutionis shown optimum field emission properties among those nanorods. Its turn-on field, threshold field, and field enhancement factor are 2.67 V/μm, 3.87 V/μm, and 1905 respectively. On the other hand, the GZO nanorods prepared with the solution of 2 % Ga/Zn molar ratio, it show the significant reduction of length, diameter, and crystalline from FE-SEM and XRD results, which will decrease the field emission properties of nanorod emitters. Therefore, the field emission measured results confirm that the gallium doped into ZnO nanorod emitters provide high carrier concentration and reduced the work function of the nanorod emitters, which exhibit lower turn-on field and threshold fields and larger field enhancement factor.

Regarding the oxygen plasma treatment, the ZnO nanorod with 60 s treatment shows the best field emission properties. The turn-on field, threshold field, and field enhancement factor are found to be 2.42 V/μm, 3.61 V/μm, and 2268 respectively. Based on Filips model, the β is approximately equal to $1+s\frac{d}{r}$, where s is dependent on screen effect, d the distance between anode and cathode and r the radius of the emitters. In our experiment, the different etched time emitters are considered with the same nanorods number density of 18.5 /μm^2 from FE-SEM images and the distance between tips and anode plate is known. Clearly, the nanorods with sharp tips have high β values. In our case, the optimum oxygen plasma etched time for the nanorods is 60 s. These nanorod emitters show lower turn-on field, uniform morphology distribution and high crystallinity. On the other hand, the ZnO nanorods with 120 s oxygen plasma treatment show decrease in aspect ratio (c/a) and destruction of nanorods from FE-SEM observation, which would degenerate the field emission properties.

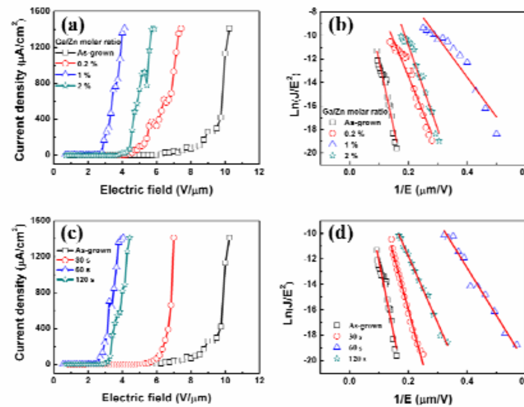

Figure 5 J-E curves and F-N plots of ((a), (b)) GZO nanorod emitters with various Ga/Zn molar

ratios in solution and ((c), (d)) ZnO nanorod emitters with various oxygen plasma treatment times.

Table1. Extracted data of the Ga/Zn atomic ratios, carrier concentration and field emission properties of GZO nanorod emitters at different Ga/Zn molar ratios in solution.

Emitters	Ga/Zn molar ratio in solution (%)	Real Ga/Zn atomic ratio of GZO nanorod based on EDS analyzed results (%)	Carrier concentration (cm^{-3})	Turn-on field (V/μm)	Threshold field (V/μm)	β value
As-grown ZnO nanorod	0	0	-	6.25	10.00	741
GZO nanorod	0.2	0.16±0.05	5.12×10^{17}	4.29	6.86	1133
	1	0.85±0.06	5.89×10^{17}	2.67	3.87	1905
	2	1.73±0.11	9.89×10^{17}	3.71	5.57	1321

Table2. The field emission properties of ZnO nanorod emitters with various oxygen plasma eching times

Emitters	Oxygen plasma bombardment time (sec)	Turn-on field (V/μm)	Threshold field (V/μm)	β value
ZnO nanorod	0	6.25	10.00	741
	30	5.17	6.83	1012
	60	2.43	3.61	2268
	120	3.00	4.14	1824

Based on the above results, we realize that the GZO nanorods (Ga/Zn molar ratio of 1 % in solution) with oxygen plasma treatment time for 60 s exhibit the optimum field emission properties. The FE-SEM images (inset in the Figure 6(a)) show the tip structure of GZO (Ga/Zn molar ratio of 1 % in solution) nanorod emitters, indicating that the GZO nanorods can be easily sharpened and exhibit a tip angle approximately 100° by oxygen plasma treatment for 60 s.

The J-E curves and F-N plots of nanorod emitters with different etched times are shown in Figures 6(a) and (b), respectively. The GZO (Ga/Zn molar ratio of 1 % in solution) nanorod emitters with tip angle of 100° have the best field emission properties among those emitters, turn-on field of 1.99 V/cm, threshold field 2.91 V/cm and field enhancement factor 2465, respectively. The comparison of field emission properties of nanorod emitters with different treatments are listed in Table 3. The results demonstrate that combination of the gallium doping and oxygen plasma treatment are able to successfully improve field emission properties of the nanorod emitters, which not only reveal the low turn-on and threshold fields and high β value but also exhibit good stability.

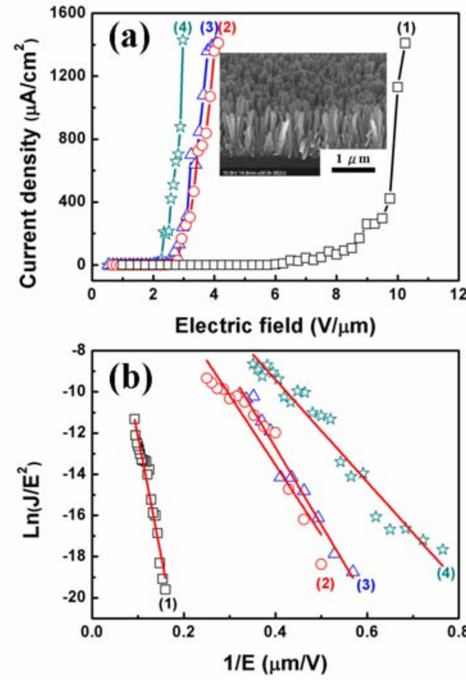

Figure 6 (a) J-E curves and (b) F-N plots of nanorod emitters with different treated processes: (1) As-grown ZnO nanorod, (2) GZO nanorod (Ga/Zn molar ratio of 1 % in solution), (3) As-grown ZnO nanorod with oxygen plasma etching for 60 sec and (4) GZO nanorod (Ga/Zn molar ratio of 1 % in solution) with oxygen plasma etching for 60 sec and the inset show the FE-SEM image of tip structure GZO nanorod emitters.

Table 3. The field emission properties of nanorod emitters with various treated processes.

Emitters	Turn-on field (V/μm)	Threshold field (V/μm)	β value
As-grown ZnO nanorod	6.25	10.00	741
GZO nanorod (Ga/Zn molar ratio of 1% in solution)	2.67	3.87	1905
As-grown ZnO nanorod+ Oxygen plasma for 60 sec	2.43	3.61	2268
GZO nanorod (Ga/Zn molar ratio of 1% in solution)+ Oxygen plasma for 60 sec	1.99	2.91	2465

Figures 7(a) and (b) depict the stability characteristics of 2×10^4 s at 25 ℃ for the tip structured GZO nanorod (Ga/Zn molar ratio of 1 % in solution) emitters and show the variations of turn-on field, threshold field and field enhancement factor are 2.01±0.09 V/μm, 3.00±0.10 V/μm and 2440.2±108.7, respectively. Figure 7(c) depicts the J-E curves for 1st, 200th, 400th and 800th operation cycles of tip structured GZO (Ga/Zn molar ratio of 1 % at solution) nanorod emitters. The stable and reproducible field emission properties can be observed up to 800 cycling tests. After the stability tests, the morphology of nanorod emitters were observed using FE-SEM and it still exhibit the nanotip on the nanorod emitters (shown in Figure 7(d)), imply the tip structure GZO nanorod emitters provide the enough lifetime and operation cycles for field emission device applications.

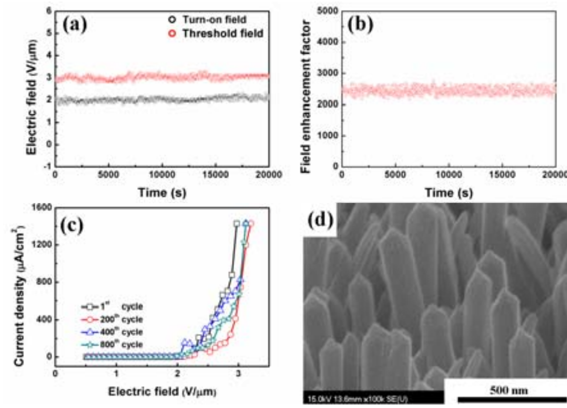

Figure 7 Stability at 25 ℃ of GZO nanorod (Ga/Zn molar ratio of 1 % in solution) with oxygen plasma etching for 60 s: (a) Turn-on and threshold fields, (b) Field emission enhanced factor, (c) 1st, 200th, 400th and 800th cycle respective J-E curves and (d) FE-SEM images of tip structured GZO nanorod emitters for stability tests.

Figure 8(a) depicts the J-E curves at temperatures of 25 ℃, 50 ℃ and 100 ℃ for tip structured GZO (Ga/Zn molar ratio of 1 % in solution) nanorod emitters. It is indicated that the nanorod emitters can be successively and stably operated between the 25 and 100 ℃. During the cycling test for 3000 s, the turn-on fields are 2.06±0.11 V/μm, 2.08±0.13 V/μm and 2.07±0.13 V/μm; the threshold fields are 3.01±0.15 V/μm, 3.07±0.16 V/μm and 3.09±0.17 V/μm; the field enhancement factor are 2442.3±97.1, 2416.0±131.0 and 2413.6±240.5 at the 25 ℃, 50 ℃ and 100 ℃, respectively, which can be calculated according to the J-E curves and they are shown in Figures 8(b)-(c).

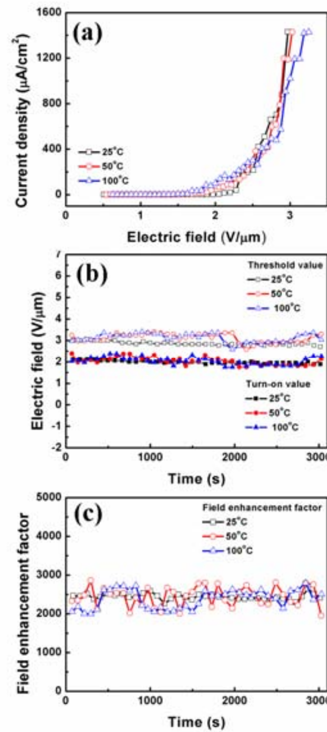

Figure 8 Stability at various temperatures of tip structure GZO nanorod emitters: (a) J-E curves, (b) Turn-on and threshold fields and (c) Field emission enhancement factor.

According to crystal defect theory, the probability (ρ) of oxygen ions to overcome the potential barrier and create vacancies can be expressed as[30]

$$\rho \approx \nu \exp(-\frac{E}{k_B T}) \quad (8)$$

where E is the potential barrier height and T the temperature. Thus, with an increase of temperature, the probability of defect formation is increased. However, in the present case, the nanorod emitters still exhibit the stable and reversible field emission properties at temperatures 25-100 ℃. Thus, oxygen plasma etching process has the advantage of obtaining more stable field emission characteristic up to 100 ℃. This phenomenon may be attributed to decreasing the concentration of oxygen vacancies of the nanorods and obtaining a better crystallinity after the treatment.

4. Conclusions

In summary, we successfully enhance the performance of ZnO employing gallium doping process and oxygen plasma treatment. The synthesized process is simple, low cost and enable to large scale production. The (002) orientation and tip-structured morphology of the nanorod emitters were proved by XRD pattern, FE-SEM and TEM observations. The PL spectrum reveals lowering the green emission peak occurred form oxygen vacancies and consequently, reduced the concentration of oxygen vacancies of the nanorod emitters after oxygen plasma treatment. The vertically aligned nanorod emitters reduce their work functions and increase electron charge carrier concentration through gallium doping process. The tip structured nanorod emitters can be formed after oxygen plasma treatment. Finally, combination of gallium doping and oxygen plasma treatment, the tip structured GZO nanorod emitters have enhanced performance including lower turn-on and threshold fields, higher field enhancement factor, good stability characteristics over 2×10^4 s at room temperature. In addition, the tip structured GZO (Ga/Zn molar ratio of 1 % in solution) nanorod emitters can be successfully and stably operated between up to 100 ℃ without notable degradation of emission properties. Therefore, the excellent field emission characteristics suggest that the tip structure ZnO nanorod emitters could be used in electron field emission and light emitting applications.

References

1. J. T. Hu, T. W. Odem, and C. M. Lieber, *Acc. Chem. Res.*, **32**, 435 (1999).
2. M. H. Huang, S. Ma, H. Feick, H. Yan, Y. Wu, H. Kind, E. Webber, R. Russo, and P. Yang, *Science*, **292**, 1987 (2001).
3. Z. H. Chen, Y. B. Tang, Y. Liu, G. D. Yuan, W. F. Zhang, J. A. Zapien, I. Bello, W. J. Zhang, C. S. Lee, and S. T. Lee, *J. Appl. Phys.*, **106**, 064303 (2009).
4. C. C. Chuang, J. H. Huang, C. C. Lee, and Y. Y. Chang, *J. Vac. Sci. Technol. B*, **23**, 772 (2005).
5. W. J. Zhang, Y. Wu, C. Y. Chan, W. K. Wang, X. M. Meng, I. Bello, Y. Lifshitz, and S. T. Lee, *Diamond Relat. Mater.*, **13**, 1037 (2004).
6. C. Y. Lee, M. P. Lu, K. F. Liao, W. W. Wu, and L. J. Chen, *Appl. Phys. Lett.*, **93**, 113109

(2008).
7. C. Y. Lee, S. Y. Li, P. Lin, and T. Y. Tseng, *IEEE Trans. On Nanotechnology*, **5**, 216 (2006).
8. C. Y. Lee, T. Y. Tseng, S. Y. Li, and P. Lin, *Nanotechnology*, **17**, 83 (2006).
9. L. F. Banerjee, S. H. Jo, and Z. F. Ren, *Adv. Mater.*, **16**, 2028 (2004).
10. Q. Wen, K. Yu, T. H. Wang, and C. L. Lin, *Appl. Phys. Lett.*, **83**, 2253 (2003).
11. U. Ozgur, Y. I. Alivov, C. Liu, A. Teke, M. A. Reshchikov, S. Dogan, V. Avrutin, S. J. Cho, and H. Morkoc, *J. Appl. Phys.*, **98**, 041301 (2005).
12. L. A. Xu, Y. Su, Y. Q. Chen, H. H. Xiao, L. A. Zhu, Q. T. Zhou, and S. Li, *J. Phys. Chem. B*, **110**, 6637 (2006).
13. X. Y. Xue, L. M. Li, H. C. Yu, Y. G. Wang, and T. H. Wang, *Appl. Phys. Lett.*, **89**, 043118 (2006).
14. S. Y. Bae, C. W. Na, J. H. Kang, and J. Park, *J. Phys. Chem. B*, **109**, 2526 (2005).
15. S. Y. Li, P. Lin, C. Y. Lee, T. Y. Tseng, and C. J. Huang, *J. Phys. D: Appl. Phys.*, **37**, 2274 (2004).
16. J. Zhong, S. Muthukumar, Y. Chen, Y. Lu, H. M. Ng, W. Jiang, and E. L. Garfunkel, *Appl. Phys. Lett.*, **83**, 3401 (2003).
17. C. Xu, M. Kim, J. Chun, and D. Kim, *Appl. Phys. Lett.*, **86**, 133107 (2005).
18. I. C. Yao, P. Lin, and T. Y. Tseng, *Nanotechnology*, **20**, 125202 (2009).
19. V. Filip, D. Nicolaescu, M. Tanemura, and F. Okuyama, *Ultramicroscopy*, **89**, 39 (2001).
20. Q. Li, V. Kumar, Y. Li, H. Zhang, J. T. Mark, and R. P. H. Chang, *Chem. Mater.*, **17**, 1001 (2005).
21. S. Ma, G. Fang, C. Li, S. Sheng, L. Fang, Q. Fu, and X. Zhao, *J. Nanosci. Nanotechno.*, **6**, 2062 (2006).
22. H. Wang, S. Baek, J. Song, J. Lee, and S. Lim, *Nanotechnology*, **19**, 075607 (2008).
23. X, Qian, H. Liu, Y. Guo, Y. Song, and Y. Li, *Nanoscale Res. Lett.,* 3, 303 (2008).
24. K. Vanhausden,W. L. Warren,C. H. Seager,D. R. Tallant,J. A. Voigt, and B. E. Gnade, *J. Appl. Phys.*, **79**, 7983(1996).
25. Y. P. Wang,W. I. Lee, and T. Y. Tseng, *Appl. Phys. Lett.*, **69**, 1807 (1996).
26. S. N. Bai, H. H. Tsai, and T. Y. Tseng, *Thin Solid Films*, **516**, 155 (2007).
27. C. X. Xu, X. W. Sun, and B. J. Chen, *Appl. Phys. Lett.*, **84**, 1540 (2004).
28. S. M. Sze, *Physics of Semiconductor Devices*, 2nd ed. (Wiley, Singapore, 1981), p. 17.
29. F. M. Charbonnier, W. A. Mackie,R. L. Hartman, and T. B. Xie, *J. Vac. Sci. Technol B*, **19**, 1064 (2001).

C. Kittel, *Introduction to Solid State Physics*, 8th ed. (Wiley, Hoboken, NJ, 2004), p. 585.